

Ultrafast X-ray Spectroscopy of Haem Proteins

Camila Bacellar^a and Majed Chergui^b

Abstract: In this article we revisit our recent picosecond and femtosecond X-ray absorption spectroscopy (XAS) and X-ray emission spectroscopy (XES) experiments, probing the ultrafast electronic and geometric evolution of photoexcited haem proteins, namely ferrous Nitrosyl Myoglobin (MbNO) and ferric Cytochrome c (Cyt c). We show through these two examples, combined with results from ultrafast optical spectroscopy, the universal behavior of the excited state dynamics of ferric and ferrous haems. Regardless of the type of ligand, its dissociation or lack thereof, or the metal oxidation state, the photoexcited system relaxes through a cascade of excited spin states leading to formation of a high spin state, which results in doming of porphyrin.

Keywords: Haem Proteins · Ultrafast Dynamics - X-ray Absorption Spectroscopy · X-ray Emission Spectroscopy · Protein Excited State Dynamics

1. Introduction

In the 1930's, Linus Pauling and co-workers found that the magnetic susceptibilities of venous (deoxygenated) and arterial (oxygenated) blood differed by a large amount (as large as 20%),^[1,2] leading them to conclude that oxyhaemoglobin and carbonmonoxyhaemoglobin contain no unpaired electrons, while ferrohaemoglobin (*i.e.* the deoxy form) contains four unpaired electrons per haem, *i.e.* the deoxy form is in a higher spin state than the ligated oxy- or carboxy-forms.

Haemoglobin (Hb) is responsible for the uptake of oxygen and its transport from the lungs to the tissues and the back transport of carbon dioxide to the lungs during the respiratory function. It is a tetramer of units, which resemble in many features to myoglobin (Mb, Figure 1a). The latter stores oxygen in muscle tissue. Haem proteins have had a special place in the development of novel spectroscopic and structural tools. Mb was the first protein whose three-dimensional structure was revealed by X-ray crystallography,^[3] soon after followed by that of haemoglobin.^[4,5] The active site (the haem, figure 1c) of both Mb and Hb is a porphyrin with an iron ion at its centre that can be either in a ferric-Fe³⁺ or ferrous-Fe²⁺ state. The ferrous form of the haem is involved in the respiratory function. On the proximal side, a histidine (His) amino-acid bound to the Fe ion links the haem porphyrin to the F helix of the protein (Figure 1a). Of course, for the respiratory function, molecular oxygen binds to the Fe²⁺ centre on the distal side of the haem. However, other ligands can also bind to the Fe centre: CO, NO in the case of ferrous haems and H₂O, CN, N₃, H₂S in the case of ferric ones, leading to different biological functions or even to malfunctions. Nitric oxide (NO) plays a role in neurotransmission, regulation of vasodilatation, platelet aggregation, and immune response.^[6–10] H₂S fulfils quite similar functions.^[11–13] It is interesting to understand how these different ligands, which do not directly enter in the respiratory function, affect the active center structure and whether and how they can be dissociated from the haem.

In the ligated form, the low-spin (LS) state of the ferrous haem can be a singlet or a doublet depending on the type of

ligand (*e.g.* CO or NO) and the haem porphyrin is in this case planar, although deviations from planarity are not uncommon. Upon ligand release from the Fe²⁺ ion, the haem switches to a HS quintet state and the pentacoordinated Fe moves out-of-plane forming the so-called domed, deoxyMb configuration. The doming occurs because going to the HS state implies populating antibonding Fe d-orbitals, which elongates the Fe-N bonds (Figure 1d). This movement of the Fe atom, in and out of the porphyrin plane, is considered the most fundamental event in the respiratory function, as it ultimately switches the haemoglobin between the so-called relaxed and tense states.^[5]

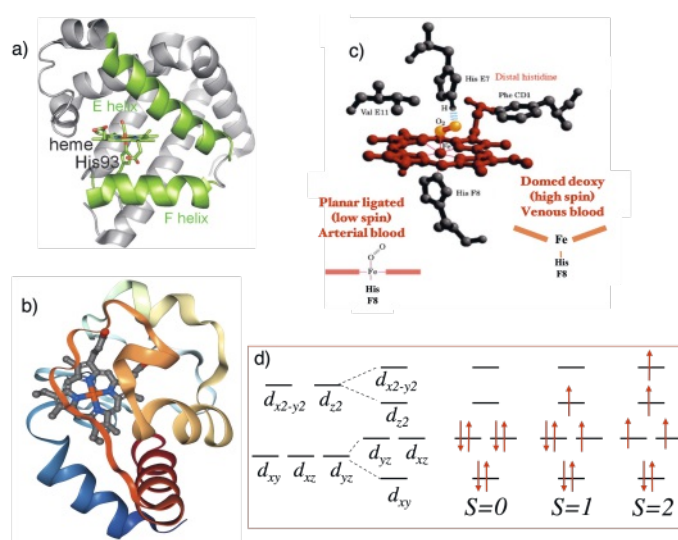


Fig. 1: a) Myoglobin. The haem iron-porphyrin has a ligand on the distal side and a histidine (His93) on the proximal side. The latter anchors the haem to the protein scaffold via the F-helix; b) cytochrome c; d) occupancy of Fe 3d-orbitals that are split by the ligand-field between bonding (d_{xy} , d_{yz} , d_{xz}) and antibonding ($d_{x^2-y^2}$, d_{z^2}) orbitals, for the different spin states of a ferrous haem.

^aCorrespondence: ^aSwissFEL, Paul-Scherrer-Institut, 5232 Villigen PSI, Switzerland

^bEcole Polytechnique Fédérale de Lausanne, Laboratoire de Spectroscopie Ultrarapide (LSU) and Lausanne Centre for Ultrafast Science (LACUS), CH-1015 Lausanne, Switzerland

Another popular class of haem proteins are the cytochromes, and in particular cytochrome c (Figure 1b), which is a small protein that mediates the electron transfer (ET) from cytochrome c reductase to cytochrome c oxidase.^[14] It also plays a role in apoptosis and its conformationally-dependent peroxidase activity.^[15,16] The active centre of Cyt c is also a haem and just as for Mb, it can occur in a ferrous or ferric form. Understanding the details of the doming motion and the return to planarity in these systems has been a focus of intense study for decades, especially using spectroscopic techniques. While ligand exchange in haem proteins is not a light-driven process, it was nevertheless shown at the end of the XIXth century that ligand photolysis of Hb upon visible-ultraviolet (visible UV) irradiation was possible.^[17] This allows to mimic the biological function of ligand detachment in a controlled fashion and monitor its return to the Fe centre.

As a consequence, the ligand dynamics in haem proteins started to be investigated as soon as time-resolved laser spectroscopic methods became available. Ligand photodissociation (CO being the most studied) and its recombination to the haem were monitored in a pump-probe scheme, first in the nanosecond,^[18] then the picosecond (ps)^[19–24] time domains. Haem proteins were also the first systems ever to be investigated by femtosecond spectroscopy.^[25–27] Furthermore, they were also the first to be investigated by Molecular Dynamics simulations.^[28] Following these pioneering studies, a huge wealth of data from simulations^[29–34] and ultrafast pump-probe studies covering various spectral ranges^[21,35–52] have been gathered on these systems with the aim of nailing down the details of the ligand detachment and recombination from and to the haem, and the accompanying transition from LS planar to HS domed and vice-versa. A great diversity of experimental observables was used, ultrafast transient absorption (TA) spectroscopy in the UV-visible being the most used approach. It monitors the dynamics of the system via the porphyrin π - π^* and n - π^* transitions,^[26,27,35,42] exploiting the significant differences in the UV-visible absorption spectrum of ligated *vs* deoxy haems. TA spectroscopy in the mid-infrared monitors the small ligands (CO, NO, H₂O, CN, N₃⁻, H₂S, *etc.*) via their stretch modes, or of the porphyrin via its high-frequency vibrational modes.^[40,41,53,54] Time-resolved resonance Raman spectroscopy is mostly sensitive to the Fe-ligand and the Fe-Histidine bond,^[55–59,37,27,43,60] or even nearby amino-acid residues, such as tryptophan.^[61,62] Finally, formation of the deoxy form upon photoexcitation of MbCO has also been reported in ps^[63,64] and fs^[65] X-ray diffraction studies.

Overall, these studies concluded that photodissociation of the diatomic ligands (CO, NO, O₂) from the planar ferrous haem porphyrin is prompt, occurring in typically <50–100 femtoseconds (fs).^[66] However, the subsequent dynamics leading to formation of the ground state HS deoxyMb form has given rise to somewhat conflicting interpretations, which can be grouped in two: namely that dissociation of the ligand generates a vibrationally hot HS state of the pentacoordinated porphyrin that then undergoes cooling, or alternatively, formation of the HS state proceeds via a cascade among electronic states of the pentacoordinated porphyrin. The latter also leads to generation of heat since the energy gap between electronic states is bridged by non-radiative transitions. While, the former scenario seemed to be generally adopted, studies during the past two decades have raised doubts about this mechanism and brought the scenario of an electronic cascade to be reconsidered.^[46,49,52] Although powerful probes of the dynamics, UV-visible, IR and Raman spectroscopies cannot intrinsically identify the nature of the electronic state (oxidation or spin state), nor can they unambiguously distinguish electronic from vibrational relaxation. In the case of ferric haems, dis-

sociation of the ligand has generally been ruled out based on observables such as the Raman response of the Fe-histidine mode upon photoexcitation and/or the absence of the free ligand stretch vibration.^[46,49,52,67] One of the key questions here is to understand to what extent the dynamics in the ferrous and ferric differ and in particular, what the role of the ligand is?

In recent years, time-resolved X-ray absorption and emission spectroscopies have emerged as ideal tools that are element-specific, can distinguish oxidation and spin state changes, and furthermore provide information on the local structure around a specific atom.^[68–70] It is interesting to note that here again, Mb was the first system ever to be investigated by time-resolved X-ray absorption spectroscopy, at that time, with microsecond resolution.^[71] One had to wait almost 30 years to see the first picosecond studies to be performed again on these systems.^[72–74] The advent of X-ray free electron lasers now enables such studies to be carried out with femtosecond resolution. In this review, we show how the combined use of ultrafast X-ray absorption and emission allows to nail down the details of the formation of the HS state and the return to the initial ligated state, lifting the ambiguities associated with the use of optical probes.

2. Ultrafast X-ray Absorption and Emission Spectroscopies

X-ray absorption spectra are characterized by absorption edges, which are due to excitation of core electrons from a given shell to the ionization threshold of a specific atom.^[68,75] They contain fine structure just below (atomic transitions), at and just above the edge (the so-called X-ray absorption near-edge structure or XANES), and well above (tens to several hundreds of eVs) the edge (the so-called extended X-ray absorption fine structure or EXAFS). The features just below the edge (or Fermi level), are due to transitions from core orbitals to unoccupied or partially filled valence orbitals. In 3d transition metals such as Fe, the K pre-edge absorption includes mainly the weak $1s \rightarrow 3d$ transitions, while the edge contains the stronger $1s \rightarrow 4p$ transitions. These transitions are especially interesting as they directly interrogate the valence orbitals involved in photoinduced dynamics, and contain information about the electronic structure (oxidation state, occupancy of valence orbitals, charge transfer, *etc.*) of the atom. The XANES region is characterised by multiple-scattering resonances of the photoelectron generated just above the ionization threshold, and they contain information about bond distances and angles, and coordination numbers. On the other hand, at even higher energies, the EXAFS modulations result from single scattering events, which deliver information about bond distances and coordination numbers of the nearest neighbours around the absorbing atom. Although simpler to analyse, EXAFS is however not commonly used in pump-probe experiments because the EXAFS modulations represent barely 10% of the edge height and scanning an extended energy range requires long data acquisitions times for each pump-probe time delay.^[68,69,75]

X-ray emission spectroscopy probes the photons emitted by an electron refilling a core hole that was created by the incident photon. It therefore reflects the density of occupied orbitals. In the case of non-resonant X-ray emission (XES), which will be the focus here, the incident photon energy is much higher than the edge energy, so that the spectral weights are largely incident energy-independent. A typical XES spectrum after ejection of an electron in the K shell consists of several emission lines^[76], shown in Figure 2a. Namely: a) the $K\alpha_1$ and $K\alpha_2$ lines, which correspond to transitions from the $2p_{3/2} \rightarrow 1s$ and $2p_{1/2} \rightarrow 1s$ orbitals, respectively, and are the most intense; b) At higher emission energies, the $K\beta_{1,3}$ lines, which are due to $3p \rightarrow 1s$ transitions. These

are nearly an order of magnitude weaker than the $K\alpha$ transitions; c) Higher still are the $K\beta_{2,3}/K\beta'$ transitions, which form the so-called valence-to-core (VtC) emission lines. They are the weakest (~ 100 times weaker than $K\alpha$) due to a poorer overlap of the initial and final wavefunctions.

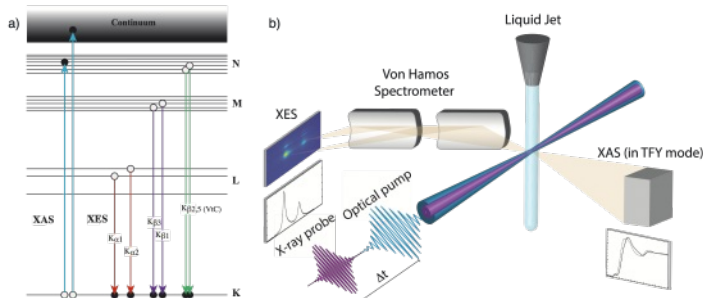


Fig. 2: (a) Absorption of X-ray photons can lead to transitions to bound (pre-edge) or continuous (above edge) states, which contain different information about the interrogated element. Following the creation of a core hole, emission can occur from different initial states, giving rise to the emission lines, which vary in cross-section and sensitivity to valence orbital dynamics. (b) Representation of a typical experimental setup used for time-resolved XAS and XES at FELs. An optical pump-pulse is used to electronically excite the sample, which is delivered in solution via a liquid jet. X-ray pulses intercept the excited system at determined time delays and the corresponding absorption and/or emission spectra are recorded as a function of time.

The $K\beta$ lines have been exploited for their sensitivity to the spin state of the emitting atom^[77] and in a pioneering experiment, fs-XES was used to track the ultrafast relaxation cascade in photoexcited an Fe(II) spin cross over (SCO) molecule.^[78] This sensitivity to the spin state stems from the exchange interaction between 3d and 3p electrons. However, it should be borne in mind that other effects also affect the $K\beta$ lines, such as covalency.^[79,80] Although the interaction between 2p and 3d orbitals is weaker than that between 3p and 3d orbitals, the $K\alpha$ lines still bear signatures of the spin state of the metal, although this is less clear cut.^[80,81] In the course of our work, we did find a systematic dependence of the $K\alpha$ line with spin, as will be detailed later.

The implementation of laser pump/X-ray probe experiments at synchrotrons has been described in several papers and will not be repeated here.^[68,69,72,82–85] The femtosecond experiments were carried out at X-ray free electron lasers (XFELs), in a pump-probe geometry, as described in refs [69,70,86–88]. Briefly, physiological solutions of the protein (ferrous MbNO and ferric Cyt C, ~ 4 mM) were delivered to the interaction region of the corresponding experiment via a recirculating liquid jet. A schematic of the setup is shown in Figure 2b. The samples are excited by an optical laser pulse and the subsequent relaxation dynamics are then probed with ultrashort X-ray pulses. In the case of XAS experiments, a monochromatized beam is scanned across the Fe K-edge in the range of ~ 7100 – 7200 eV and absorption spectra are recorded in total fluorescence yield mode (TFY). For XES experiments, the full SASE beam is used well above the absorption edge (8000–9300 eV) and the emitted photons are dispersed by a spectrometer in the von Hamos geometry onto a 2D detector. In both measurements, the X-ray signals are recorded at twice the repetition rate of the laser source, such that an unpumped reference is interleaved with every other pumped shot. Changing the relative arrival time between the optical laser and the X-rays allows us to follow the excited state evolution as a function of time.

3. Results

3.1 Picosecond and Femtosecond X-ray Absorption Experiments

We carried out steady-state XANES studies of myoglobin both in deoxy form and ligated with the ligands CO, NO, CN, O₂ and H₂O.^[89] A detailed analysis of the electronic and molecular structure at the Fe site was provided, which confirmed the domed character of the deoxy form, in accord with previous crystallographic studies. These steady-state XANES studies served as the basis for the time-resolved ones, which were carried out at synchrotrons with 70 ps temporal resolution.^[72,74] Figure 3a shows the Fe K-edge steady-state spectrum of MbNO and a typical transient spectrum, which exhibits a similar profile to Fe K-edge transients of other Mb's.^[72,73,90] It has to be mentioned that quite similar profiles have been reported for photoexcited ferrous cytochrome c (Cyt c)⁹¹ and ferric Cyt c,^[88] as discussed below and shown in Figure 3b. Indeed, the transient is the difference between the ground and excited-state absorptions, this profile can be quite well reproduced by taking the difference of the deoxy steady-state spectrum minus that of the ligated protein, also shown in Figure 3a. This confirms that in all cases, the dominant feature on the transient XANES spectra is the Fe-N bond elongation leading to the doming of the Fe ion out of the porphyrin plane. More recently, our fs X-ray experiments^[88,92] showed that the initial doming motion indeed occurs immediately following photoexcitation, within the ~ 130 fs instrument response function, which can be observed in the rise time of the signal at 7122.5 eV in the case of MbNO. The same behaviour was observed for ferric Cyt c reflecting, for the first time, a doming of the porphyrin in a ferric system, even though the methionine ligand is not considered to be photodissociated from the Fe atom.^[67] This settles a long debate as to whether doming is a viable option ferric hemes,^[93] and we can conclude that doming is a universal deformation in the response of haem systems to photoexcitation.

In the case of ferrous haems, for which ligand photodissociation occurs, rebinding of the ligand to the haem iron is a central issue, as it mimics the natural binding process. It is challenging to unambiguously identify this process in the XANES transient spectra due to overlapping spectral contributions from ligated and unligated haems (the quantum yield for ligand photodissociation is 1 only in the case of MbCO), which may have different kinetics, and the competition between in-pocket recombination and recombination with ligands that have left the haem pocket. In the case of MbNO, the weak deviations between the experimental transient and the difference spectrum of the steady-state spectra in Figure 3a, are real and have been extensively analysed in ref. ^[74]. They were attributed to formation of a domed-ligated species, which had been postulated on the basis of optical TA studies^[94] and simulations.^[30,31] This is most evident at ~ 7135 eV, which also underscores the difficulty of distinguishing the different species by XAS. Our preliminary results using fs XANES at XFELs do not contradict this observation,^[95] and do not have a sufficient signal-to-noise ratio across the necessary energy range to confirm it either. Future experiments will aim at observing a time-dependent spectral change in the ligand-binding sensitive region as a way to fully capture the ligand dissociation and subsequent recombination.

In Cytochrome c, observation of ligand dissociation is even more challenging, since there are no XAS spectra of stable pentacoordinated deoxy Cyt c species, such as deoxyMb, that one could compare to the excited spectra in order to facilitate the assignment. Cyt c does not bind diatomic molecules, but rather a methionine residue on its sixth coord-

Table 1: Comparison of the rise (τ_r) and decay times (τ) reported different ferric and ferrous haem proteins, using various spectroscopic techniques. The attribution of time scales is discussed in the text without. All time constants are in picoseconds.

Species	Method	τ_r	τ_1	τ_2	τ_3
Ferric Cyt c ⁸⁸	XAS, XES	0.15	0.62±0.06		8.2±4
Ferric Cyt c ^{50,51}	UV-Vis TA and fluo.	<0.05	0.7±0.09	3.4±0.3	11±2
Ferric MetMb ^{52,100}	UV-Vis TA	<0.08	0.51	1.14	4.8
Ferric MbCN ⁴⁶	UV-Vis-IR TA	< 0.05	0.3		3
Ferric MbN ₃ ⁴⁹	IR TA			2.4	18
Ferrous Cyt c ^{50,51}	UV-Vis TA and fluo.	<0.05	0.6±0.06	1.8 ± 0.5	5.9 ± 0.1
Ferrous MbCO ¹⁰¹	XAS	<0.07	0.4		msec
Ferrous MbNO ⁹²	XAS, XES	<0.1	0.6		30

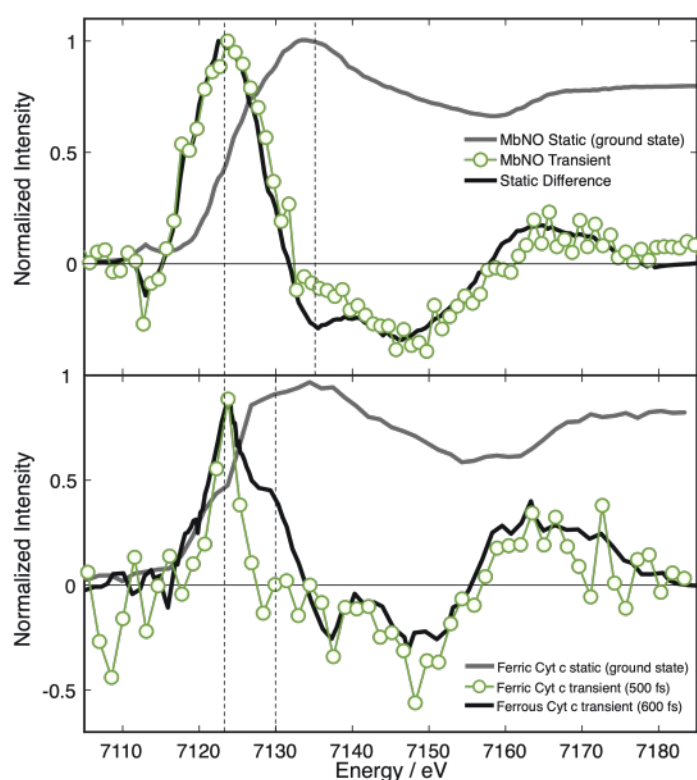


Fig. 3: (a) Static (grey) and transient (excited minus unpumped) spectrum of MbNO at 70 ps (green dots) and static difference between ground state MbNO and deoxyMb (black);^[74] (b) Static (grey line) and transient spectra of Ferric Cyt c at 500 fs (green dots)^[88] and of ferrous Cyt c at 600 fs (black line) from ref. 91, both measured at XFELs. The dashed lines refer to the energies mentioned in the main text.

dination site. Upon photoexcitation, ferrous Cyt c is known to undergo dissociation of the Fe-S bond, much like in ferrous Mb's.^[43, 44, 50, 51, 67] This was supported by X-ray absorption and emission measurements performed by Mara *et al.* at the LCLS XFEL (Stanford).^[91] Using MXAN simulations^[96] to fit their XANES spectra, they established that the distance of the methionine from the Fe atom is greater than 2.9 Å after photoexcitation, pointing to its dissociation from the Fe centre. However, our ferric Cyt c transient XANES exhibits a quite similar profile to ferrous Cyt c (Figure 3b), which mostly reflects haem doming. While this does not rule out ligand dissociation, the significant deviation of the transient signal at around 7130 eV could point to the bound ligand in the ferric case. This is especially relevant as doming has always been considered to result from ligand dissociation. The existence of domed ligated species, as observed for MbNO, suggests that these two processes can occur independently in haem systems. Future experiments aim to focus on an alternative probe to the methionine dissociation by monitoring the dynamics using S K-edge absorption (near 2.5 keV), in order to unambiguously verify the occurrence of methionine dissociation or lack thereof.

In summary, transient XANES experiments provide already a great deal of insight into the structural deformations incurred by the haem upon photoexcitation and point to doming as a universal process regardless of the oxidation state and the occurrence of ligand dissociation or lack of it. However, at this stage, transient XAS does not provide information about the electronic mechanism that leads to doming, which is best captured by X-ray emission spectroscopy (XES).

3.2 Femtosecond Non-Resonant X-ray Emission Studies

Although a certain degree of structural information is contained in XES spectra,^[76,79] it is strongly dominated by electronic effects and is therefore predominantly sensitive to the electronic and spin structure. As mentioned above, $K\beta$ emission is particularly known for its sensitivity to the spin state.^[78] We implemented fs XES to follow the haem relaxation after photoexcitation of MbNO^[92] and Figure 4 shows the relevant transients for both $K\alpha$ and $K\beta$ lines. The interpretation of these transient signals is achieved using a combination of model systems and simulations. In ref. ^[78], model systems with similar geometry and electronic configuration, at specific spin states serve to generate a “static difference” to emulate the expected transient signals in photoexcited species. Using the same approach, we have shown that the recovery of the ground state of MbNO implies the passage through two HS states, which can be distinguished spectrally. In Figure 4a, the top panel shows the transient spectra of $K\beta$ lines at short (260 fs), intermediate (500 fs) and longer (1.3 ps) time delays, while the bottom panel shows the difference spectra expected for a doublet to quintet and doublet to triplet states from model systems. The region between 7050 and 7055 eV contains a strong fingerprint of the different HS states, with the transition to the quintet state showing intensity depletion in this range. The transient spectra show very similar features, such that we can identify the initial transition to a triplet state followed by relaxation to a quintet state. The shape of the difference spectra stays constant from >1 ps, until complete recovery of the ground state.

The dependence of the $K\alpha$ emission with spin is less well established^[80,81] than for $K\beta$, and reference spectra of intermediate spin compounds are not available. Therefore, we performed density functional theory (DFT) calculations to simulate the transitions to triplet and quintet states (lower panel, Figure 4b). Here, we also see a difference between short and long-time delays, more specifically in the $K\alpha_2$ line, around 639 eV. These features agree with those observed in the DFT simulations, further confirming that the relaxation proceeds via a fast decay through an intermediate HS quintet state. The kinetic traces show a rise of ~ 800 fs, associated with the decay from the triplet state to the quintet state, which relaxes back to the ground state in a biexponential fashion, associated with the relaxation

of HS deoxyMb-NO species from geminate ($\tau \sim 30$ ps) and non-geminate ($\tau \sim 1.5$ ns) ligand recombination.^[74]

In order to obtain similar information for ferric cytochrome c, one needs to investigate even higher spin intermediate states, namely, transitions to the quartet and sextet states. It was shown that the $K\alpha$ line-shape does not change significantly for spins beyond $S=3/2$,^[81] making the identification of intermediate species much more complicated. It is possible, however, to focus on the valuable information contained in the kinetic traces. The time evolution of the transient XES $K\alpha$ signal shows a bi-exponential decay, with the same time constants as obtained in the XAS measurements. Considering that the XES is a pure electronic signature and is not sensitive to vibrational effects, we can conclude that these time scales reflect an electronic relaxation among spin states. Looking more carefully at the normalized transient spectra shown in Figure 5a, one can notice that the positive peak at 6406 eV and the negative one at 6404 eV of the $K\alpha_1$ transient show somewhat different temporal evolution. Selecting specific regions of interest (ROIs) around each of these features and plotting the intensity of each signal as a function of time, we recover two different kinetic traces, which are shown in Figure 5b. The negative ROI kinetics shows a prompt rise followed by a biexponential decay, while the positive feature shows a slower rise and a mono-exponential decay. The fast decay of the negative component closely matches that of the rise of the positive peak, suggesting a cascade process in which an intermediate state (presumably, a quartet state) feeds population into the HS sextet state. The assignment of HS states of $S>3/2$ is also confirmed by $K\beta$ transient spectra, but in this case, the S/N was not sufficient to unambiguously assign a specific transition. This analysis reveals that $K\alpha$ spectra contain more information about the spin states than previously thought, warranting further investigation for a more general class of metal complexes.

The general picture that emerges from the above results is that for haem proteins (ferric or ferrous) the return to the ground state is characterised by a cascade among spin state and is not due to cooling of the pentacoordinated species in its HS ground state. This behaviour goes beyond just the two systems discussed here (MbNO and ferric Cyt c) as a common pattern for all investigated haem proteins. This is illustrated in Table I, which presents the relaxation times reported

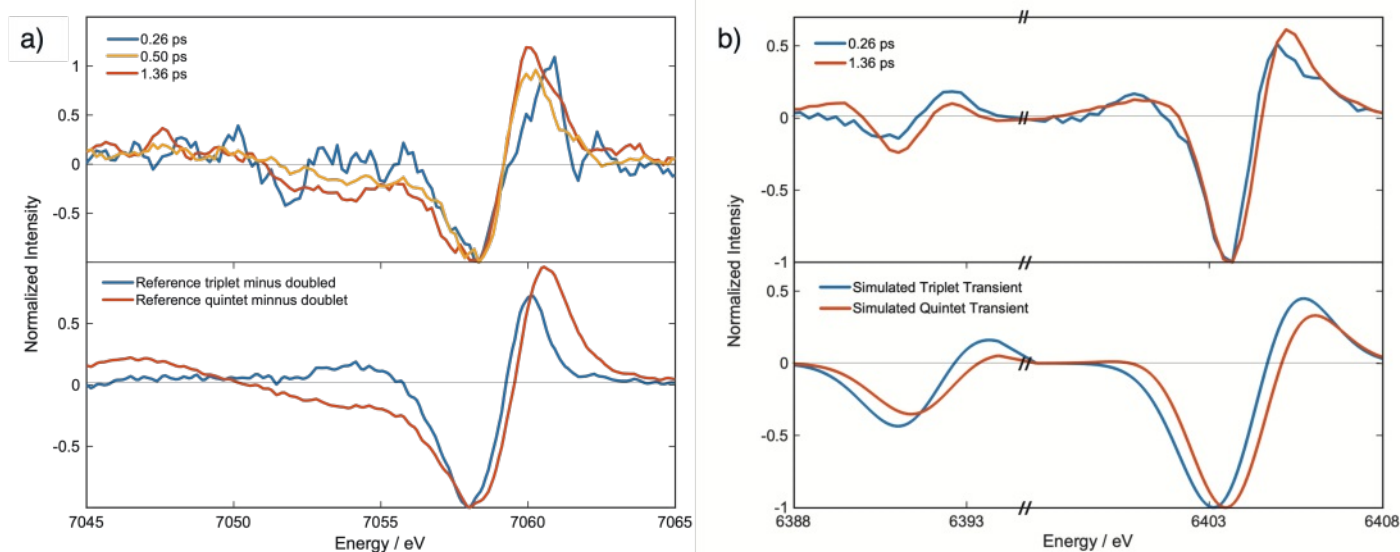


Figure 4: (a) top: Transient XES $K\beta$ spectra of MbNO at delays of 0.26 (blue), 0.5 (yellow) and 1.36 ps (red). Bottom: Difference of steady-state XES $K\beta$ spectra from Fe complexes (ref): triplet minus doublet (blue), quintet minus doublet (red). (b) top: Transient $K\alpha$ XES spectra of MbNO at 0.26 (blue) and 1.36 ps (red). Bottom: difference $K\alpha$ spectra derived from DFT simulations, triplet minus doublet (blue), quintet minus doublet (red). Experimental spectra and simulations are reproduced from reference.92

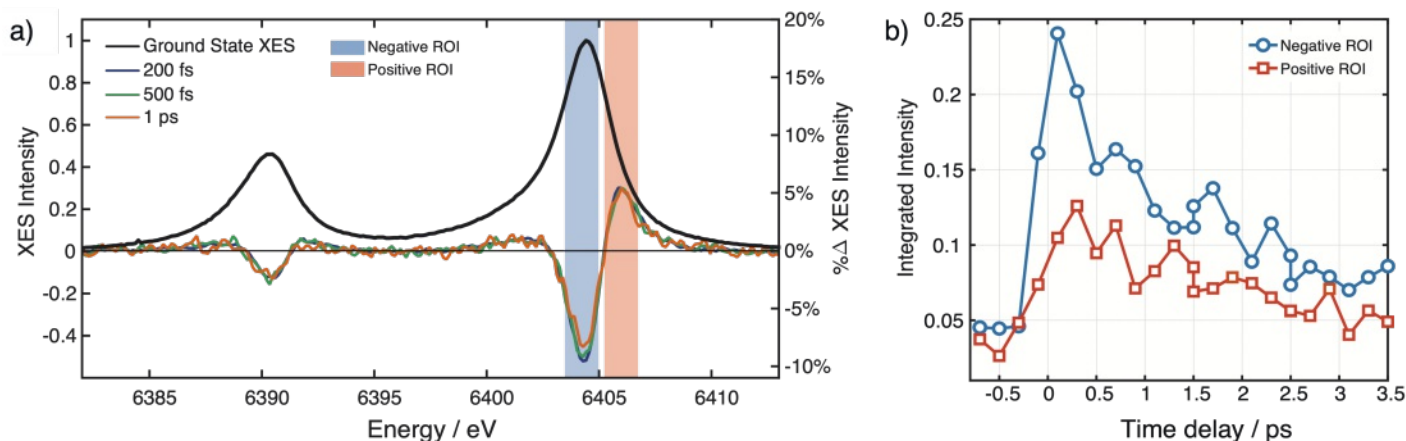


Fig. 5: (a) Static (black) and representative normalized transient (coloured) XES spectra of Cyt c at different time delays from 200 fs to 1 ps. The blue and red shaded areas represent the regions of interest (ROIs) used for integration of the transient spectra. (b) Kinetic traces obtained from the integration of the positive (red squares) and negative (blue circles) ROIs, showing that the different regions present different dynamics.⁸⁸

in optical and the more recent X-ray TA studies and in the fs XES studies. Evidently, the non-radiative cascade will generate heat in the systems as has unambiguously established in transient IR^[46,53] and time-resolved Raman studies.^[61,97,98] The energy-gap between low, intermediate and high spin states is not known as accessing them from the LS GS is both dipole- and spin-forbidden (these are dd-excitations). However, resonant X-ray emission spectroscopy, also called resonant inelastic X-ray scattering (RIXS) can give access to these. This approach boils down to an electronic Raman process. A RIXS study of MbCN, metMb, MbCO and deoxyMb was reported by Harada *et al.*^[99] showing for the first three occurrence of at least 2 states below the Q-bands of the porphyrin, which lie at an energy loss of ~ 1.5 and ~ 0.5 eV, while for deoxyMb mainly one main feature is observed at an energy of ~ 0.8 eV. The latter most likely corresponds to the intermediate spin state in MbNO, while the former would correspond to the intermediate and HS states of ferric Cyt c. While this is speculative and needs further investigation, the important message is that the intermediate dd-excitations are separated by relatively large energy gaps, rather than being at thermal energies.^[49] It is important to stress that the cascade among spin states is strongly borne out by the XES data presented here, because it is not sensitive to thermal effects.

We believe this is a common behaviour of all ferric and ferrous systems and the results presented here show the universality of the photoexcitation dynamics of this class of proteins. This is shown in Figure 6, where the shortest (rise) time τ_r corresponds to the formation of the intermediate spin state from the initially excited $\pi-\pi^*$ and $n-\pi^*$ of the porphyrin. τ_1 corresponds to the decay of the intermediate to the state and τ_3 corresponds to the decay of the HS state returning to the initial ground state. This timescale varies greatly between the various haem proteins and is strongly influenced by the steric and electronic effects of the surrounding protein environment and the nature of the ligand. τ_2 is most probably due to vibrational relaxation in the HS state, and it also depends on the environment and the interaction with the ligand. It does not show up in the X-ray spectroscopic studies because XAS and XES are not sensitive to vibrational effects.

4. Conclusions

In this short review, we have revisited our recent picosecond and femtosecond X-ray absorption and emission results on the photoinduced dynamics in ferrous Myoglobin-NO and ferric cytochrome c casting them in a broader picture of the spin cross-over dynamics in haem proteins. In summary, the

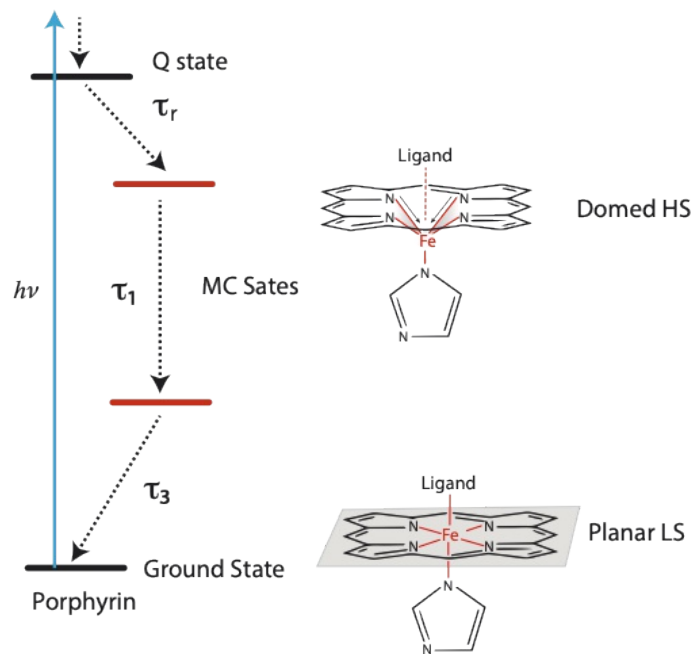


Fig. 6: Generic scheme of the relaxation pathways of photoexcited ferrous and ferric haems. τ_r is the relaxation from the $\pi-\pi^*$ excited porphyrin to the intermediate spin state due to population of metal d-orbitals. τ_1 is the relaxation from the intermediate to the lowest high spin state and τ_3 is the return to the initial ground state. A τ_2 component is also present, which is due to thermal relaxation in the HS state (see Table I and text).

message we wish to convey is that in all ferrous haem proteins, the formation of the high spin deoxyMb species is entirely governed by a cascade among spin states, and the return to the planar low-spin form is also a spin transition. We believe this settles a long-standing controversy about the importance of thermal vs electronic effects in the formation of the deoxy form for ferrous haems. It also shows that even in ferric haems, for which ligand dissociation is ruled out, a spin cascade occurs leading to formation of a domed species. Of course, a spin cascade does not rule out additional thermal effects since the energy between states is dissipated non-radiatively to the protein.

Overall, the presented X-ray spectroscopic studies^[88,92,95] of MbNO and Cyt c underscore the importance of selecting the experimental observable one uses in order to probe the dynamics of photoexcited in haem proteins. These observables along with those of IR^[41,53,54] and visible^[35] transient absorp-

tion spectroscopy, fluorescence up-conversion^[50,100] and resonance Raman spectroscopy^[43,67] are crucial for the emergence of a complete picture of ligand dynamics in proteins.

Acknowledgments

This work was supported by the Swiss NSF via the NCCR: MUST and grants 200020_169914 and 200021_175649 and the European Research Council Advanced Grant H2020 ERCEA 695197 DYNAMOX. We are very grateful to our collaborators from the EPF-Lausanne, the SwissFEL and SLS (PSI-Villigen), the SACLA XFEL (Japan) and the FXE team at Eu-XFEL (Hamburg) for their great contributions to the results presented herein.

Received: May 1, 2022

- [1] L. Pauling and C. D. Coryell, *Proc. Natl. Acad. Sci. U.S.A.* **1936**, 22, 210, <https://doi.org/10.1073/pnas.22.4.210>.
- [2] L. Pauling and C. D. Coryell, *PNAS* **1936**, 22, 159, <https://doi.org/10.1073/pnas.22.3.159>.
- [3] J. C. Kendrew, G. Bodo, H. M. Dintzis, R. G. Parrish, H. Wyckoff and D. C. Phillips, *Nature* **1958**, 181, 662, <https://doi.org/10.1038/181662a0>.
- [4] M. F. Perutz, M. G. Rossmann, A. F. Cullis, H. Muirhead, G. Will and A. C. T. North, *Nature* **1960**, 185, 416, <https://doi.org/10.1038/185416a0>.
- [5] M. F. Perutz, A. J. Wilkinson, M. Paoli and G. G. Dodson, *Annu. Rev. Biophys. Biomol. Struct.* **1998**, 27, 1, <https://doi.org/10.1146/annurev.biophys.27.1.1>.
- [6] C. Nathan, *FASEB J.* **1992**, 6, 3051, <https://doi.org/10.1096/fasebj.6.12.1381691>.
- [7] S. Moncada and A. Higgs, *N. Engl. J. Med.* **1993**, 329, 2002, <https://doi.org/10.1056/NEJM199312303292706>.
- [8] R. G. Knowles, M. Palacios, R. M. J. Palmer and S. Moncada, *P. Natl. Acad. Sci. U.S.A.* **1989**, 86, 5159, <https://doi.org/10.1073/pnas.86.13.5159>.
- [9] J. S. Stamler, D. J. Singel and J. Loscalzo, *Science* **1992**, 258, 1898, <https://doi.org/10.1126/science.1281928>.
- [10] L. Jia, C. Bonaventura, J. Bonaventura and J. S. Stamler, *Nature* **1996**, 380, 221, <https://doi.org/10.1038/380221a0>.
- [11] L. Li and P. K. Moore, *Trends Pharmacol. Sci.* **2008**, 29, 84, <https://doi.org/10.1016/j.tips.2007.11.003>.
- [12] C. Chen, H. Xin and Y. Zhu, *Acta Pharmacol. Sin.* **2007**, 28, 1709, <https://doi.org/10.1111/j.1745-7254.2007.00629.x>.
- [13] R. Pietri, A. Lewis, R. G. León, G. Casabona, L. Kiger, S.-R. Yeh, S. Fernandez-Alberti, M. C. Marden, C. L. Cadilla and J. López-Garriga, *Biochemistry* **2009**, 48, 4881, <https://doi.org/10.1021/bi801738j>.
- [14] G. R. Moore and G. W. Pettigrew, *Cytochromes c: evolutionary, structural and physicochemical aspects*, Springer Ser. Mol. Cell. Biol. **2012**.
- [15] X. Liu, C. N. Kim, J. Yang, R. Jemerson and X. Wang, *Cell* **1996**, 86, 147, [https://doi.org/10.1016/S0092-8674\(00\)80085-9](https://doi.org/10.1016/S0092-8674(00)80085-9).
- [16] N. A. Belikova, Y. A. Vladimirov, A. N. Osipov, A. A. Kapralov, V. A. Tyurin, M. V. Potapovich, L. V. Basova, J. Peterson, I. V. Kurnikov and V. E. Kagan, *Biochemistry* **2006**, 45, 4998, <https://doi.org/10.1021/bi0525573>.
- [17] J. Haldane and J. L. Smith, *J. Physiol.* **1896**, 20, 497, <https://doi.org/10.1113/jphysiol.1896.sp000634>.
- [18] B. Alpert, S. El Mohsni, L. Lindqvist and F. Tibbel, *Chem. Phys. Lett.* **1979**, 64, 11, [https://doi.org/10.1016/0009-2614\(79\)87265-6](https://doi.org/10.1016/0009-2614(79)87265-6).
- [19] L. J. Noe, W. G. Eisert and P. M. Rentzepis, *Proc. Natl. Acad. Sci. U.S.A.* **1978**, 75, 573, <https://doi.org/10.1073/pnas.75.2.573>.
- [20] B. I. Greene, R. M. Hochstrasser, R. B. Weisman and W. A. Eaton, *Proc. Natl. Acad. Sci. U.S.A.* **1978**, 75, 5255, <https://doi.org/10.1073/pnas.75.11.5255>.
- [21] D. A. Chernoff, R. M. Hochstrasser and A. W. Steele, *Proc. Natl. Acad. Sci. U.S.A.* **1980**, 77, 5606, <https://doi.org/10.1073/pnas.77.10.5606>.
- [22] P. A. Cornelius, A. W. Steele, D. A. Chernoff and R. M. Hochstrasser, *PNAS* **1981**, 78, 7526, <https://doi.org/10.1073/pnas.78.12.7526>.
- [23] P. A. Cornelius, R. M. Hochstrasser and A. W. Steele, *J. Mol. Biol.* **1983**, 163, 119, [https://doi.org/10.1016/0022-2836\(83\)90032-3](https://doi.org/10.1016/0022-2836(83)90032-3).
- [24] S. M. Janes, G. A. Dalickas, W. A. Eaton and R. M. Hochstrasser, *Biophys. J.* **1988**, 54, 545, [https://doi.org/10.1016/S0006-3495\(88\)82987-4](https://doi.org/10.1016/S0006-3495(88)82987-4).
- [25] C. Shank, E. Ippen and R. Bersohn, *Science* **1976**, 193, 50, <https://doi.org/10.1126/science.935853>.
- [26] J. Martin, A. Migus, C. Poyart, Y. Lecarpentier, R. Astier and A. Antonetti, *Proc. Natl. Acad. Sci.* **1983**, 80, 173, <https://doi.org/10.1073/pnas.80.1.173>.
- [27] J. W. Petrich, C. Poyart and J. Martin, *Biochemistry* **1988**, 27, 4049, <https://doi.org/10.1021/bi00411a022>.
- [28] D. A. Case and M. Karplus, *J. Mol. Biol.* **1979**, 132, 343, [https://doi.org/10.1016/0022-2836\(79\)90265-1](https://doi.org/10.1016/0022-2836(79)90265-1).
- [29] J. E. Straub and M. Karplus, *Chem. Phys.* **1991**, 158, 221, [https://doi.org/10.1016/0301-0104\(91\)87068-7](https://doi.org/10.1016/0301-0104(91)87068-7).
- [30] M. Meuwly, O. M. Becker, R. Stote and M. Karplus, *Biophys. Chem.* **2002**, 98, 183, [https://doi.org/10.1016/S0301-4622\(02\)00093-5](https://doi.org/10.1016/S0301-4622(02)00093-5).
- [31] D. Nutt and M. Meuwly, *Biophys. J.* **2005**, 88, 46A.
- [32] M. Devereux and M. Meuwly, *Biophys. J.* **2009**, 96, 4363, <https://doi.org/10.1016/j.bpj.2009.01.064>.
- [33] K. El Hage, S. Brickel, S. Hermelin, G. Gaulier, C. Schmidt, L. Bonacina, S. C. van Keulen, S. Bhattacharyya, M. Chergui, P. Hamm, U. Rothlisberger, J.-P. Wolf and M. Meuwly, *Struct. Dyn.* **2017**, 4, 061507, <https://doi.org/10.1063/1.4996448>.
- [34] J. W. Petrich, J. C. Lambry, K. Kuczera, M. Karplus, C. Poyart and J. L. Martin, *Biochemistry*, **1991**, 30, 3975, <https://doi.org/10.1021/bi00230a025>.
- [35] J. L. Martin and M. H. Vos, *Annu. Rev. Biophys. Biomol. Struct.* **1992**, 21, 199, <https://doi.org/10.1146/annurev.bb.21.060192.001215>.
- [36] J.-L. Martin and M. H. Vos, *Methods Enzymol. Academic Press*, **1994**, 232, 416, [https://doi.org/10.1016/0076-6879\(94\)32057-8](https://doi.org/10.1016/0076-6879(94)32057-8).
- [37] S. Dasgupta, T. G. Spiro, C. K. Johnson, G. A. Dalickas and R. M. Hochstrasser, *Biochemistry* **1985**, 24, 5295, <https://doi.org/10.1021/bi00341a003>.
- [38] Y. Kholodenko, M. Volk, E. Gooding and R. M. Hochstrasser, *Chem. Phys.* **2000**, 259, 71, [https://doi.org/10.1016/S0301-0104\(00\)00182-8](https://doi.org/10.1016/S0301-0104(00)00182-8).
- [39] Y. Kholodenko, E. A. Gooding, Y. Dou, M. Ikeda-Saito and R. M. Hochstrasser, *Biochemistry* **1999**, 38, 5918, <https://doi.org/10.1021/bi983022v>.
- [40] S. Kim, G. Jin and M. Lim, *J. Phys. Chem.* **2004**, 108, 20366, <https://doi.org/10.1021/jp0489020>.
- [41] J. Kim, J. Park, T. Lee and M. Lim, *J. Phys. Chem.* **2012**, 116, 13663, <https://doi.org/10.1021/jp308468j>.
- [42] X. Ye, A. A. Demidov, F. Rosca, W. Wang, A. Kumar, D. Ionascu, D. Barick, D. Wharton, P. M. Champion, *J. Phys. Chem.* **2003**, 107, 40, 8156, <https://doi.org/10.1021/jp0276799>.
- [43] S. Berezina, H. Wohlrab and P. M. Champion, *Biochemistry* **2003**, 42, 614, <https://doi.org/10.1021/bi027387y>.
- [44] W. Wang, X. Ye, A. A. Demidov, F. Rosca, T. Sjodin, W. Cao, M. Sheeran and P. M. Champion, *J. Phys. Chem.* **2000**, 104, 10789, <https://doi.org/10.1021/jp0008602>.
- [45] C. Ferrante, E. Pontecorvo, G. Cerullo, M. Vos and T. Scopigno, *Nat. Chem.* **2016**, 8, 1137, <https://doi.org/10.1038/nchem.2569>.
- [46] J. Helbing, L. Bonacina, R. Pietri, J. Bredenbeck, P. Hamm, F. van Mourik, F. Chaussard, A. Gonzalez-Gonzalez, M. Chergui, C. Ramos-Alvarez, C. Ruiz and J. Lopez-Garriga, *Biophys. J.* **2004**, 87, 1881, <https://doi.org/10.1529/biophysj.103.036236>.
- [47] M. H. Vos, *Biochim. Biophys. Acta, Bioenerg.* **2008**, 1777, 15, <https://doi.org/10.1016/j.bbabi.2007.10.004>.
- [48] U. Liebl, J.-C. Lambry and M. H. Vos, *Biochim. Biophys. Acta, Proteins Proteomics* **2013**, 1834, 1684, <https://doi.org/10.1016/j.bbapap.2013.02.025>.
- [49] J. Helbing, *Chem. Phys.* **2012**, 396, 17, <https://doi.org/10.1016/j.bbapap.2013.02.025>.
- [50] O. Bram, C. Consani, A. Cannizzo and M. Chergui, *J. Phys. Chem.* **2011**, 115, 13723, <https://doi.org/10.1021/jp207615u>.
- [51] C. Consani, O. Bram, F. van Mourik, A. Cannizzo and M. Chergui, *Chem. Phys.* **2012**, 396, 108, <https://doi.org/10.1016/j.chemphys.2011.09.002>.
- [52] C. Consani, G. Aubeck, O. Bram, F. van Mourik and M. Chergui, *J. Chem. Phys.* **2014**, 140, <https://doi.org/10.1063/1.4861467>.
- [53] M. Lim, T. A. Jackson and P. A. Anfirud, *J. Phys. Chem.* **1996**, 100, 12043, <https://doi.org/10.1021/jp9536458>.
- [54] M. Lim, T. A. Jackson and P. A. Anfirud, *J. Am. Chem. Soc.* **2004**, 126, 7946, <https://doi.org/10.1021/ja035475f>.
- [55] J. Terner, J. D. Stong, T. G. Spiro, M. Nagumo, M. Nicol and M. A. El-Sayed, *PNAS* **1981**, 78, 1313, <https://doi.org/10.1073/pnas.78.3.1313>.
- [56] E. W. Findsen, J. M. Friedman, M. R. Ondrias and S. R. Simon, *Science* **1985**, 229, 661, <https://doi.org/10.1126/science.4023704>.
- [57] E. W. Findsen, T. W. Scott, M. R. Chance, J. M. Friedman and M. R. Ondrias, *J. Am. Chem. Soc.* **1985**, 107, 3355, <https://doi.org/10.1021/ja00297a056>.
- [58] E. W. Findsen and M. R. Ondrias, *J. Am. Chem. Soc.* **1984**, 106, 19, 5736, <https://doi.org/10.1021/ja00331a059>.
- [59] J. M. Friedman, M. R. Ondrias, E. W. Findsen and S. R. Simon, *P. Soc. Photo-Opt. Inst.* **1985**, 533, 8.
- [60] S. G. Kruglik, B. K. Yoo, S. Franzen, M. H. Vos, J. L. Martin and M. Negrerie, *P. Natl. Acad. Sci. U.S.A.* **2010**, 107, 13678, <https://doi.org/10.1073/pnas.0912938107>.
- [61] Y. Mizutani and T. Kitagawa, *Science* **1997**, 278, 443, <https://doi.org/10.1126/science.278.5337.443>.
- [62] T. Kitagawa, N. Haruta and Y. Mizutani, *Biopolymers* **2002**, 67, 207, <https://doi.org/10.1002/bip.10096>.
- [63] F. Schotte, M. Lim, T. A. Jackson, A. V. Smirnov, J. Soman, J. S. Olson, G. N. Phillips, M. Wulff and P. A. Anfirud, *Science* **2003**, 300, 1944, <https://doi.org/10.1126/science.1078797>.

- [64] G. Hummer, F. Schotte and P. A. Anfinrud, *Proc. Natl. Acad. Sci. U.S.A.* **2004**, *101*, 15330, <https://doi.org/10.1073/pnas.0405295101>.
- [65] T. R. M. Barends, L. Foucar, A. Ardevol, K. Nass, A. Aquila, S. Botha, R. B. Doak, K. Fahahati, E. Hartmann, M. Hilpert, M. Heinz, M. C. Hoffmann, J. Kofinger, J. E. Koglin, G. Kovacsova, M. Liang, D. Milathianaki, H. T. Lemke, J. Reinstein, C. M. Roome, R. L. Shoeman, G. J. Williams, I. Burghardt, G. Hummer, S. Boutet and I. Schlichting, *Science* **2015**, *350*, 445, <https://doi.org/10.1126/science.aac5492>.
- [66] P. M. Champion, F. Rosca, D. Ionascu, W. X. Cao and X. Ye, *Faraday Discuss.* **2004**, *127*, 123, <https://doi.org/10.1039/b316440c>.
- [67] M. Negrerie, S. Cianetti, M. H. Vos, J.-L. Martin and S. G. Kruglik, *J. Phys. Chem. B* **2006**, *110*, 12766, <https://doi.org/10.1021/jp0559377>.
- [68] M. Chergui, *Acta Crystallogr. A* **2010**, *66*, 229, <https://doi.org/10.1107/S010876730904968X>.
- [69] C. J. Milne, T. J. Penfold and M. Chergui, *Coordin. Chem. Rev.* **2014**, *277*, 44, <https://doi.org/10.1016/j.ccr.2014.02.013>.
- [70] M. Chergui and E. Collet, *Chem. Rev.* **2017**, *117*, 11025, <https://doi.org/10.1021/acs.chemrev.6b00831>.
- [71] D. M. Mills, A. Lewis, A. Harootunian, J. Huang and B. Smith, *Science* **1984**, *223*, 811, <https://doi.org/10.1126/science.223.4638.811>.
- [72] F. A. Lima, C. J. Milne, D. C. V. Amarasinghe, M. H. Rittmann-Frank, R. M. van der Veen, M. Reinhard, V. T. Pham, S. Karlsson, S. L. Johnson, D. Grolimund, C. Borca, T. Huthwelker, M. Janousch, F. van Mourik, R. Abela and M. Chergui, *Rev. Sci. Instrum.* **2011**, *82*, <https://doi.org/10.1063/1.3600616>.
- [73] A. B. Stickrath, M. W. Mara, J. V. Lockard, M. R. Harpham, J. Huang, X. Zhang, K. Attenkofer and L. X. Chen, *J. Phys. Chem. B* **2013**, *117*, 4705, <https://doi.org/10.1021/jp3086705>.
- [74] M. Silatani, F. A. Lima, T. J. Penfold, J. Rittmann, M. E. Reinhard, H. M. Rittmann-Frank, C. Borca, D. Grolimund, C. J. Milne and M. Chergui, *PNAS* **2015**, *112*, 12922, <https://doi.org/10.1073/pnas.1424446112>.
- [75] C. Bressler and M. Chergui, *Annu. Rev. Phys. Chem.* **2010**, *61*, 263, <https://doi.org/10.1146/annurev.physchem.012809.103353>.
- [76] P. Glatzel and U. Bergmann, *Coordin. Chem. Rev.* **2005**, *249*, 65, <https://doi.org/10.1016/j.ccr.2004.04.011>.
- [77] G. Vankó, T. Neisius, G. Molnár, F. Renz, S. Kárpáti, A. Shukla and F. M. F. de Groot, *J. Phys. Chem. B* **2006**, *110*, 11647, <https://doi.org/10.1021/jp0615961>.
- [78] W. Zhang, R. Alonso-Mori, U. Bergmann, C. Bressler, M. Chollet, A. Galler, W. Gawelda, R. G. Hadt, R. W. Hartsock, T. Kroll, K. S. Kjær, K. Kubiček, H. T. Lemke, H. W. Liang, D. A. Meyer, M. M. Nielsen, C. Purser, J. S. Robinson, E. I. Solomon, Z. Sun, D. Sokaras, T. B. van Driel, G. Vankó, T.-C. Weng, D. Zhu and K. J. Gaffney, *Nature* **2014**, *509*, 345, <https://doi.org/10.1038/nature13252>.
- [79] C. J. Pollock, M. U. Delgado-Jaime, M. Atanasov, F. Neese and S. DeBeer, *J. Am. Chem. Soc.* **2014**, *136*, 9453, <https://doi.org/10.1021/ja504182n>.
- [80] S. Lafuerza, A. Carluantonio, M. Retegan and P. Glatzel, *Inorg. Chem.* **2020**, *59*, 12518, <https://doi.org/10.1021/acs.inorgchem.0c01620>.
- [81] J. Kawai, C. Suzuki, H. Adachi, T. Konishi and Y. Gohshi, *Phys. Rev. B* **2004**, *50*, 11347–11354, <https://doi.org/10.1103/PhysRevB.50.11347>.
- [82] C. Bressler, R. Abela and M. Chergui, *Z. Kristallogr.* **2008**, *223*, 307, <https://doi.org/10.1524/zkri.2008.0030>.
- [83] C. Bressler, M. Saes, M. Chergui, D. Grolimund, R. Abela and P. Pattison, *J. Chem. Phys.* **2002**, *116*, 2955, <https://doi.org/10.1063/1.1435618>.
- [84] M. Saes, F. van Mourik, W. Gawelda, M. Kaiser, M. Chergui, C. Bressler, D. Grolimund, R. Abela, T. E. Glover, P. A. Heimann, R. W. Schoenlein, S. L. Johnson, A. M. Lindenberg and R. W. Falcone, *Rev. Sci. Instrum.* **2003**, *75*, 24, <https://doi.org/10.1063/1.1633003>.
- [85] L. X. Chen, *Annu. Rev. Phys. Chem.* **2005**, *56*, 221, <https://doi.org/10.1146/annurev.physchem.56.092503.141310>.
- [86] M. Chergui, *Struct. Dyn.* **2016**, *3*, 031001, <https://doi.org/10.1063/1.4953104>.
- [87] C. J. Milne, T. Schietinger, M. Aiba, A. Alarcon, J. Alex, A. Anghel, V. Arsov, C. Beard, P. Beaud and S. Bettoni, *Appl. Sci.* **2017**, *7*, 720.
- [88] C. Bacellar, D. Kinschel, G. F. Mancini, R. A. Ingle, J. Rouxel, O. Cannelli, C. Cirelli, G. Knopp, J. Szlachetko, F. A. Lima, S. Menzi, G. Pamfilidis, K. Kubiček, D. Khakhulin, W. Gawelda, A. Rodriguez-Fernandez, M. Biednov, C. Bressler, C. A. Arrell, P. J. M. Johnson, C. J. Milne and M. Chergui, *Proc. Natl. Acad. Sci. U.S.A.* **2020**, *117*, 21914, <https://doi.org/10.1073/pnas.2009490117>.
- [89] F. A. Lima, T. J. Penfold, R. M. van der Veen, M. Reinhard, R. Abela, I. Tavernelli, U. Rothlisberger, M. Benfatto, C. J. Milne and M. Chergui, *Phys. Chem. Chem. Phys.* **2014**, *16*, 1617, <https://doi.org/10.1039/C3CP53683A>.
- [90] M. L. Shelby, A. Wildman, D. Hayes, M. W. Mara, P. J. Lestranger, M. Cammarata, L. Balducci, M. Artamonov, H. T. Lemke, D. Zhu, T. Seideman, B. M. Hoffman, X. Li and L. X. Chen, *Proc. Natl. Acad. Sci. U.S.A.* **2021**, *118*, <https://doi.org/10.1073/pnas.2018966118>.
- [91] M. W. Mara, R. G. Hadt, M. E. Reinhard, T. Kroll, H. Lim, R. W. Hartsock, R. Alonso-Mori, M. Chollet, J. M. Glowonia, S. Nelson, D. Sokaras, K. Kunnus, K. O. Hodgson, B. Hedman, U. Bergmann, K. J. Gaffney and E. I. Solomon, *Science*, **2017**, *356*, 1276, <https://doi.org/10.1126/science.aam6203>.
- [92] D. Kinschel, C. Bacellar, O. Cannelli, B. Sorokin, T. Katayama, G. F. Mancini, J. R. Rouxel, Y. Obara, J. Nishitani, H. Ito, T. Ito, N. Kurahashi, C. Higashimura, S. Kudo, T. Keane, F. A. Lima, W. Gawelda, P. Zalden, S. Schulz, J. M. Budarz, D. Khakhulin, A. Galler, C. Bressler, C. J. Milne, T. Penfold, M. Yabashi, T. Suzuki, K. Misawa and M. Chergui, *Nat. Commun.* **2020**, *11*, 4145, <https://doi.org/10.1038/s41467-020-17923-w>.
- [93] R. J. Sension, *Proc. Natl. Acad. Sci. U.S.A.*, **2020**, *117*, 26550, <https://doi.org/10.1073/pnas.2017806117>.
- [94] D. Ionascu, F. Gruia, X. Ye, A. Yu, F. Rosca, C. Beck, A. Demidov, J. S. Olson and P. M. Champion, *J. Am. Chem. Soc.* **2005**, *127*, 16921, <https://doi.org/10.1021/ja054249y>.
- [95] C. Bacellar, D. Kinschel, O. Cannelli, B. Sorokin, T. Katayama, G. F. Mancini, J. Rouxel, Y. Obara, J. Nishitani, H. Ito, T. Ito, N. Kurahashi, C. Higashimura, S. Kudo, C. Cirelli, G. Knopp, K. Nass, P. J. M. Johnson, A. Wach, J. Szlachetko, F. Lima, C. J. Milne, M. Yabashi, T. Suzuki, K. Misawa and M. Chergui, *Faraday Discuss.* **2021**, *228*, <https://doi.org/10.1039/D0FD00131G>.
- [96] M. Benfatto, A. Congiu-Castellano, A. Daniele and S. D. Longa, *J. Synchrotron. Radiat.* **2001**, *8*, 267, <https://doi.org/10.1107/S0909049500015338>.
- [97] Y. Mizutani, Y. Uesugi and T. Kitagawa, *J. Chem. Phys.* **1999**, *111*, 8950, <https://doi.org/10.1063/1.480253>.
- [98] N. Fujii, M. Mizuno and Y. Mizutani, *J. Phys. Chem. B* **2011**, *115*, 13057, <https://doi.org/10.1021/jp207500b>.
- [99] Y. Harada, M. Taguchi, Y. Miyajima, T. Tokushima, Y. Horikawa, A. Chainani, Y. Shiro, Y. Senba, H. Ohashi, H. Fukuyama and S. Shin, *J. Phys. Soc. Jpn.* **2009**, *78*, 044802, <https://doi.org/10.1143/JPSJ.78.044802>.
- [100] O. Bräm, A. Cannizzo and M. Chergui, *J. Phys. Chem. A* **2019**, *123*, 1461, <https://doi.org/10.1021/acs.jpca.9b00007>.
- [101] M. Levantino, H. T. Lemke, G. Schirò, M. Glowonia, A. Cupane and M. Cammarata, *Struct. Dyn.* **2015**, *2*, 041713, <https://doi.org/10.1063/1.4921907>.

License and Terms



This is an Open Access article under the terms of the Creative Commons Attribution License CC BY 4.0. The material may not be used for commercial purposes.

The license is subject to the CHIMIA terms and conditions: (<https://chimia.ch/chimia/about>).

The definitive version of this article is the electronic one that can be found at <https://doi.org/10.2533/chimia.2022.538>